ACS OMEGA

http://pubs.acs.org/journal/acsodf

Article

Quantum Chemical Exploration of A−π_1−D_1−π_2−D_2-Type Compounds for the Exploration of Chemical Reactivity, Optoelectronic, and Third-order Nonlinear Optical Properties

Ghulam Mustafa, Iqra Shafiq, Qurat-ul-ain Shaikh, Ayesha Mustafa, Romaisa Zahid, Faiz Rasool,* Muhammad Adnan Asghar, Rabia Baby, Saad M. Alshehri, and Muhammad Haroon

Cite This: *ACS Omega* 2023, 8, 22673−22683

Read Online

ACCESS | Metrics & More | Article Recommendations | Supporting Information

ABSTRACT: Organic compounds exhibit significant nonlinear optical (NLO) properties and can be utilized in various areas like optical parameters, fiber optics, and optical communication. Herein, a series of chromophores (**DBTD1**−**DBTD6**) with an A−π_1−D_1−π_2−D_2 framework was derived from a prepared compound (**DBTR**) by varying the structure of π-spacer and terminal acceptor. The **DBTR** and its investigated compounds were optimized at the M06/6-311G(d,p) level of theory. Frontier molecular orbitals (FMOs), nonlinear optical (NLO) properties, global reactivity parameters (GRPs), natural bonding orbital (NBO), transition density matrix (TDM), molecular electrostatic potential (MEP), and natural population analysis (NPA) were accomplished at the abovementioned level to describe the NLO findings. **DBTD6** has the lowermost band gap (2.131 eV) among all of the derived compounds. The decreasing order of highest occupied molecular orbital−lowest unoccupied molecular orbital (HOMO−LUMO) energy gap values was **DBTR** > **DBTD1** > **DBTD2** > **DBTD3** > **DBTD4** > **DBTD5** > **DBTD6**. The NBO analysis was carried out to describe noncovalent interactions such as conjugative interactions and electron delocalization. From all of the examined substances, **DBTD5** showed the highest λ_{max} value at 593.425 nm (in the gaseous phase) and 630.578 nm (in chloroform solvent). Moreover, the β_{tot} and $\langle\gamma\rangle$ amplitudes of **DBTD5** were noticed to be relatively greater at 1.140×10^{-27} and 1.331×10^{-32} esu, respectively. So, these outcomes disclosed that **DBTD5** depicted the highest linear and nonlinear properties in comparison to the other designed compounds, which underlines that it could make a significant contribution to hi-tech NLO devices.

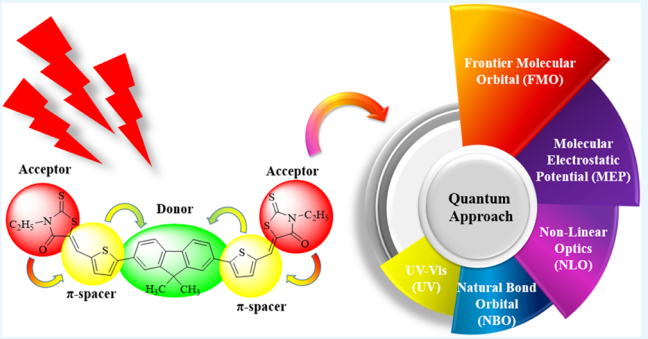

INTRODUCTION

The modification of the optical characteristics of a substance's structure in the presence of photons or light exhibits a macroscopic phenomenon called nonlinear optics (NLO).[1] In recent decades, multiple enhancements regarding NLO have been made in the data transformation, electro-optics, fiber optics, photonic lasers, and data storage disciplines.[2] Moreover, the telecommunications sector has been extensively developed owing to the potential employment of second-order NLO materials, which exhibit ultrafast signal transmission via electro-optic modulation.[3] The most prominent characteristics of NLO compounds are broadly categorized as their conjugated molecular framework, amplitude, optical frequency, phase, and polarizable nature.[4] Researchers have put tremendous effort into both theoretical and experimental exploration of different classes of NLO materials, including NLO polymers, molecular dyes, organic as well as inorganic semiconductors, and nanomaterials.[5−7]

Following the development, organic NLO compounds have been extensively studied considering the presence of many proficient features like an extendable π-conjugated system,[8] remarkable photothermal stability, flexibility in molecular structure, durability, novel optic, electronic spectra, large NLO susceptibility, quick response time, and ease in structural designing and modulation.[9−11] Conventionally, semimetal NLO materials, mainly silicon based, have been employed in quantum dots, batteries, and photosensitized solar cells.[12] While moving a step ahead in computational modulation, polymer-based NLO materials emerged as a very promising area of research contrary to their semimetal counterparts.[13]

It is well known that conducting-type polymers are used in the synthetic process of medical equipment such as inhalers,[14]

Received: March 4, 2023
Accepted: May 31, 2023
Published: June 12, 2023

transistors,[15] and most specifically field-effect transistors.[16,17] In accordance with the manufacturing domain, they are also potentially employed in electrochromic materials, smart windows, light-emitting diodes (LEDs), optical data storage, solar cells, and shielding materials.[18−20] Most of the recently developed NLO polymers have a guest−host configuration of chromophores immersed in the polymer matrix or covalently attached to the chains of the polymer. It is noted that the nonlinearity in the optical properties is associated with the chromophore substituent on the polymer chain, encompassing excellent NLO response.[21]

Furthermore, the NLO properties of these organic systems are strongly influenced by the delocalization of electric charge across the π-conjugated network. The configuration pattern of NLO chromophores involves the interaction of donor and acceptor through π-spacers. The electronic charge delocalization happens from donor to acceptor moieties via π-linker beyond hurdle, generating first- and second-order nonlinear responses as well as the dipole nonlinearity.[22−24] Efficient assembly of donor, π-spacer, and acceptor moieties contributes solely to enhance the intramolecular charge transfer (ICT), which is also taken as an impactful strategy while tuning NLO response properties.[25−28] Numerous studies successfully reported that the listed techniques, such as extended delocalization through π-linkage; metal−ligand structural framework; incorporation of an electronic charge network; assimilation of a suitable donor, π-spacer, and acceptor unit; and bond-length alteration, are employed to achieve better NLO properties.[29]

The current computational investigation is expected to improve electronic charge delocalization by utilizing different lengths of π-spacers in the entitled derivatives. It is noticed from the literature that among all of the conducting polymers, polyanilines are of high interest owing to their remarkable stability and exceptional conduction process.[30,31] The functional groups attached to the polymer's backbone are responsible for these intriguing properties along with their electrical properties. Thus, functionalized conduction polymers (polyanilines) are potentially endorsed by the scientific community and have been reported significantly in the literature as suitable NLO candidates.[32]

Herein, **Flu-RH** is being taken as a parent compound that was recently synthesized *via* the Suzuki coupling mechanism, where rhodanine dye has been incorporated at both ends of the fluorine backbone.[33] In this work, **Flu-RH** is transformed into **DBTR** via side-chain modifications. The rhodanine moiety at one end is replaced by *N*,*N*-dimethylaniline and a varied number of aniline moieties are introduced in each new derivative. This series of derivatives is subjected to density functional theory (DFT) (NLO and NBO study) and time-dependent density functional theory (TD-DFT) (frontier molecular orbitals (FMOs), transition density matrices (TDMs), density of state (DOS), global reactivity parameters (GRPs), absorption spectrum (UV−vis), and hole−electron analyses) approaches at the M06 level of theory and 6-311G(d,p) basis set. Moreover, the NLO response of said chromophores is estimated in terms of hyperpolarizabilities, UV−visible spectra, and HOMO/LUMO diagrams with the utilization of corrected long-range hybrid DFT methods, and the computed results are displayed in their respective sections. Through structural modification with various efficient donor, spacer, and acceptor units, the efficacy of optoelectronic materials significantly improved. Therefore, it is expected that the current study will open ways to synthesize rhodanine-dye-based compounds having enhanced NLO behavior.

RESULTS AND DISCUSSION

In this work, the NLO properties of **DBTR** and **DBTD1**−**DBTD6** have been investigated to develop promising NLO materials. We utilized (5*Z*,5′*Z*)-5,5′-(((9,9-dimethyl-9*H*-fluorene-2,7-diyl)bis(thiophene-5,2-diyl))bis(methaneylylidene))-bis(3-ethyl-2-thioxothiazolidin-4-one) abbreviated as **DBTR** as a reference compound with A−π−D−π−A configuration. A series of designed chromophores with A−π_1−D_1−π_2−D_2 architecture is made by the structural modulation of **DBTR** (Figure 1). First, **DBTD1** is designed by changing one end-capped acceptor with *N*,*N*-dimethylaniline (donor moiety) and thiophene (π-spacer) with *N*1-methyl-*N*4-(*p*-tolyl) benzene-1,4-diamine. **DBTD1**−**DBTD6** are designed by the addition of *N*1-methyl-*N*4-(*p*-tolyl) benzene-1,4-diamine (monomer) in each derivative. The ChemDraw structures of these studied chromophores are depicted in Figure 2 and their IUPAC names are presented in Table S34. Furthermore, Figure S3 presents the optimized structures of these molecules, while their Cartesian coordinates are tabulated in Tables S1−S7. It is estimated that this research will be very useful for the synthesis of high-efficacy NLO materials.

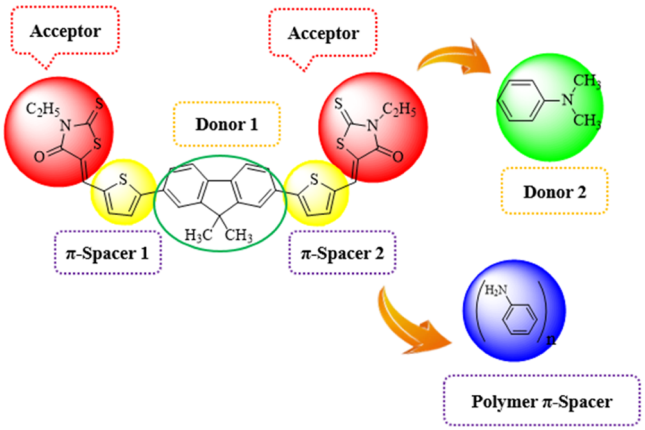

Figure 1. Sketch map of designed compounds (**DBTD1**−**DBTD6**) from reference (**DBTR**).

Frontier Molecular Orbitals (FMOs). FMO analysis is an effective way to investigate electronic transitions, chemical stability, and reactivity of a molecule.[34−37] The HOMO (highest occupied molecular orbital) and the LUMO (lowest unoccupied molecular orbital) of a system have a significant impact on the optical and electrical properties of molecules by using the HOMO−LUMO band gap.[38−40] LUMO expresses the capacity to accept electrons, whereas HOMO depicts the potential to donate electrons.[41,42] Molecules showing large ICT usually offer the best NLO response.[43,44]

The E_{HOMO} and E_{LUMO} of designed chromophores (**DBTD1**−**DBTD6**) are computed at the M06/6-311G(d,p) level, and the outcomes are presented in Table 1, while the energies of higher orbitals (E_{HOMO-1}, E_{LUMO+1}, E_{HOMO-2}, and E_{LUMO+2}) are tabulated in Table S8. All of the designed chromophores (**DBTD1**−**DBTD6**) display a lower energy gap ($E_{gap} = E_{LUMO} - E_{HOMO}$) in contrast to the reference chromophore (**DBTR**) (Figure S4). Theoretically calculated

https://doi.org/10.1021/acsomega.3c01472
ACS Omega 2023, 8, 22673−22683

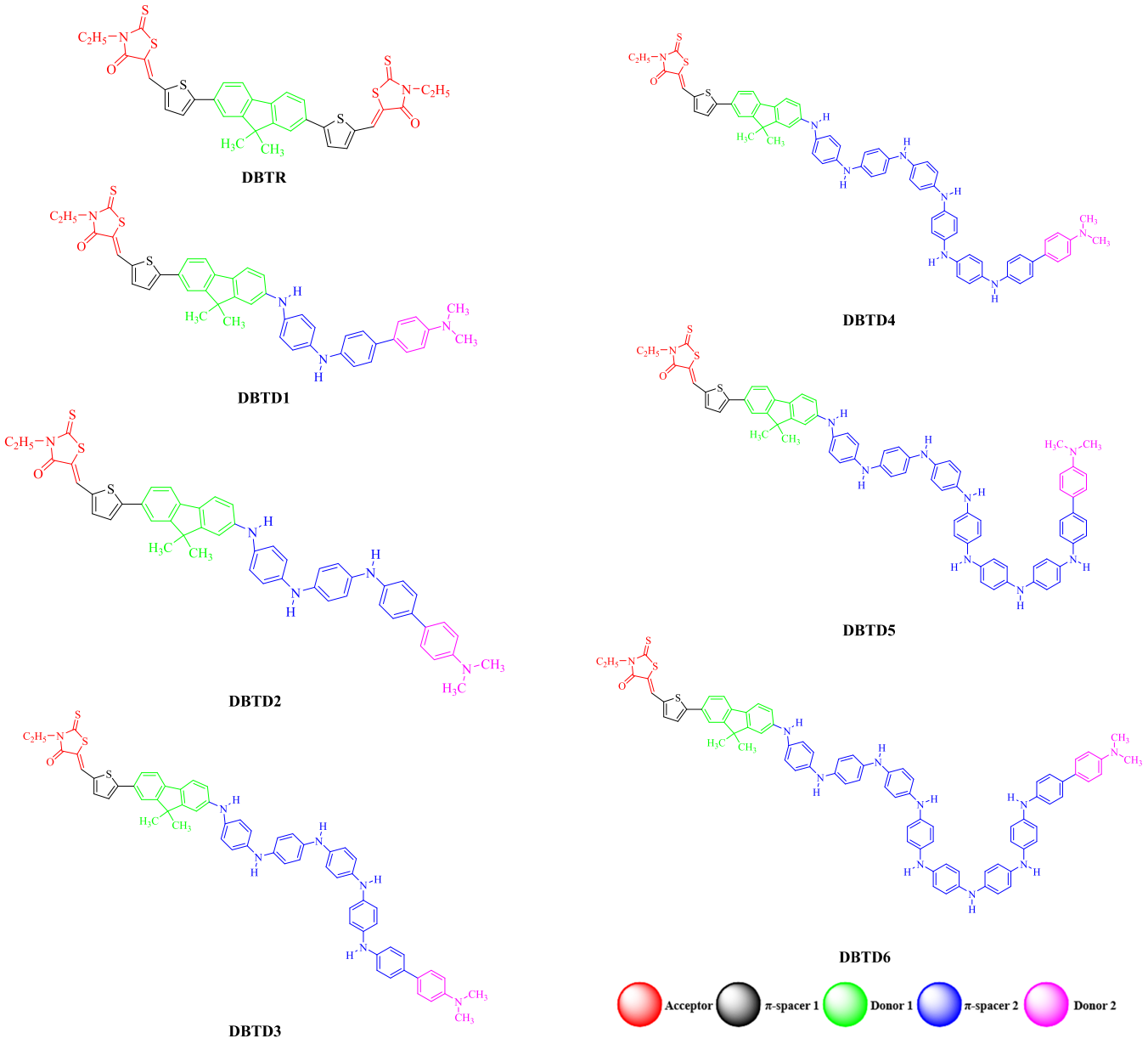

Figure 2. ChemDraw structures of investigated moieties (**DBTR** and **DBTD1**−**DBTD6**).

Table 1. E_{HOMO}, E_{LUMO}, and Energy Gap (ΔE) of the Entitled Species[a]

compounds	E_{HOMO}	E_{LUMO}	band gaps
DBTR	−5.937	−2.867	3.070
DBTD1	−5.177	−2.680	2.497
DBTD2	−5.041	−2.682	2.359
DBTD3	−4.897	−2.675	2.222
DBTD4	−4.866	−2.670	2.196
DBTD5	−4.814	−2.676	2.138
DBTD6	−4.797	−2.666	2.131

[a]Units in eV.

values of E_{HOMO} and E_{LUMO} of **DBTR** are −5.937 and −2.867 eV, respectively, with a 3.070 eV band gap.

For **DBTD1**−**DBTD6**, the observed E_{HOMO}/E_{LUMO} values are −5.177/−2.680, −5.041/−2.682, −4.897/−2.675, −4.866/−2.670, −4.814/−2.676, and −4.797/−2.666 eV, respectively. Moreover, the observed energy gaps for **DBTD1**−**DBTD6** are 2.497, 2.359, 2.222, 2.196, 2.138, and 2.131 eV, respectively. A reduction in ΔE is noticed in all of the designed chromophores due to a higher level of HOMO and a lower level of LUMO, which deliver a high intramolecular charge transfer (ICT).

The reference compound has a higher energy gap value than all of the derivatives. This band gap is lowered to 2.497 eV in **DBTD1** because of the development of a strong push−pull phenomenon that is accompanied by structural variation, i.e., by swapping the terminal acceptor by the *N*,*N*-dimethylaniline donor unit (D2) and the thiophene ring with N1-methyl-N4-(p-tolyl) benzene-1,4-diamine (π-spacer 2). The energy gap is further reduced in **DBTD2** and **DBTD3** (2.359 and 2.222 eV) due to the addition of three and five aniline monomers (which act as π-linkers), respectively. Thus, the conjugation of the system is improved by increasing π-linkers, which reduces the energy gap. Frontier molecular orbitals of **DBTR** and **DBTD1**−**DBTD6** are depicted in Figure S1.

Due to the addition of six, seven, and eight aniline monomers in **DBTD4**−**DBTD6**, the band gap is further decreased (2.196−

https://doi.org/10.1021/acsomega.3c01472
ACS Omega 2023, 8, 22673−22683

2.131 eV). **DBTD6** has the lowest band gap among all of the studied species due to an increase in resonance and conjugation, which is attributed to the addition of eight aniline π-linkers. The ascending order of the HOMO−LUMO energy gap is as follows: **DBTD6** > **DBTD5** > **DBTD4** > **DBTD3** > **DBTD2** > **DBTD1** > **DBTDR**. This pattern shows that the continuous addition of aniline would be influential in achieving remarkable NLO behavior.

To support the above calculations, we also studied the FMO diagrams to realize the charge-transfer processes resulting from the density distribution among the ground and excited states. In **DBTDR**, the electronic cloud of HOMO and LUMO is primarily located throughout the molecule. However, in **DBTD1−DBTD6**, the majority of the charge density for HOMO is focused above the π-spacer (π_1) and donor (D_2); only a small amount of it lies on the donor (D_1), while for LUMO, a greater quantity of charge has existed on the π-spacer (π_2). The same phenomenon of ICT between higher orbitals is shown in Figure S1. This electronic charge reinforcement indicates that all of the designed molecules are competent NLO active compounds.

Absorption Analysis. To evaluate the optical properties, UV−vis absorption spectra of **DBTR** and **DBTD1−DBTD6** are computed in the gaseous and solvent phases. The maximum absorption wavelength (λ_{max}), excitation energy (E), oscillator strength (f_{os}), and molecular orbital (MO) assistances of **DBTR** and **DBTD1−DBTD6** are shown in Tables S9−S22, and their spectral details are depicted in Figure 3. Additionally, six-state transitions of **DBTR** and **DBTD1−DBTD6** are shown in Tables S9−S22 in the solvent and gaseous phases. It is observed that enhanced conjugation in addition to an electron-withdrawing peripheral unit displays the greatest bathochromic shift in the UV−visible spectrum.[45,46] Our designed species having A−π_1−D_1−π_2−D_2 configuration and extended π-conjugation exhibit a wide range of absorption wavelengths.

Tables S9−S22 display that the computed values of λ_{max} for **DBTR** and **DBTD1−DBTD6** are found in the range of 485.641−593.425 nm in the gaseous phase and 508.945−630.578 nm in the solvent phase (chloroform). **DBTD5** has the highest λ_{max} at 593.425 and 630.578 nm with excitation energies of 2.089 and 1.966 eV in the gaseous phase and chloroform, respectively. The highest λ_{max} is due to the presence of seven aniline π-linkers, which boost the conjugation as well as lower the band gap sandwiched between the ground and excited states and give rise to a bathochromic shift resulting in better optical properties. **DBTR** demonstrates the lowest λ_{max} values at 485.641 and 508.945 nm with 2.553 and 2.436 eV excitation energies in gas and chloroform, respectively. The decreasing order of λ_{max} values in the gas phase is **DBTD5** > **DBTD6** > **DBTD4** > **DBTD3** > **DBTD2** > **DBTD1** > **DBTR**, with values of 593.425 > 584.638 > 577.584 > 575.012 > 558.840 > 533.931 > 485.641 nm. Likewise, the declining trend of λ_{max} values in chloroform is **DBTD5** > **DBTD6** > **DBTD3** > **DBTD4** > **DBTD2** > **DBTD1** > **DBTR** with values of 630.578 > 626.246 > 616.745 > 615.642 > 591.274 > 569.990 > 508.945 nm. To summarize the entire discussion, these compounds are excellent NLO materials for use in optoelectronics due to their high absorption wavelength and high charge transferability.

Global Reactivity Parameters (GRPs). Global reactivity parameters (GRPs) are used to accurately determine stability, chemical reactivity, and several other factors.[47,54−56] Using ΔE data, determined from FMOs, the GRPs envisage the chemical potential (μ), ionization potential (IP), electron affinity (EA),

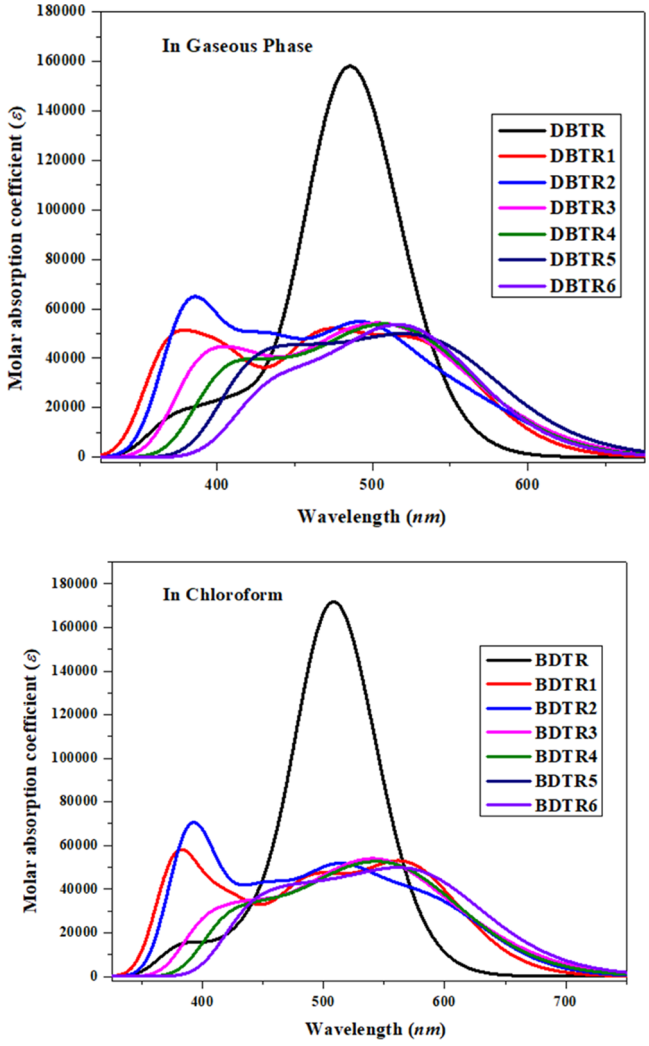

Figure 3. UV−vis absorption spectra of investigated molecules **DBTR** and **DBTD1−DBTD6**.

global softness (σ), electronegativity (X), global hardness (η), and electrophilicity index (ω) of the examined species. These values are calculated by using eqs 1−7[48−52] and results are tabulated in Table 2.

$$\mathrm{IP} = -E_{\mathrm{HOMO}} \tag{1}$$

$$\mathrm{EA} = -E_{\mathrm{LUMO}} \tag{2}$$

$$X = -\frac{[E_{\mathrm{LUMO}} + E_{\mathrm{HOMO}}]}{2} \tag{3}$$

$$\eta = -\frac{[E_{\mathrm{LUMO}} - E_{\mathrm{HOMO}}]}{2} \tag{4}$$

$$\mu = \frac{E_{\mathrm{HOMO}} + E_{\mathrm{LUMO}}}{2} \tag{5}$$

$$\sigma = \frac{1}{2\eta} \tag{6}$$

$$\omega = \frac{\mu^2}{2\eta} \tag{7}$$

Ionization potential (IP) and electron affinity (EA) measurements can be used to quantify an object's capacity to donate

https://doi.org/10.1021/acsomega.3c01472
ACS Omega 2023, 8, 22673−22683

Table 2. Global Reactivity Descriptors of DBTR and DBTD1−DBTD6[a]

compounds	IP	EA	X	η	μ	ω	σ
DBTR	5.937	2.867	4.402	1.535	−4.402	6.311	0.325
DBTD1	5.177	2.680	3.929	1.249	−3.928	6.180	0.400
DBTD2	5.041	2.682	3.862	1.179	−3.861	6.328	0.423
DBTD3	4.897	2.675	3.786	1.111	−3.786	6.450	0.450
DBTD4	4.866	2.670	3.768	1.098	−3.768	6.465	0.455
DBTD5	4.814	2.676	3.745	1.069	−3.745	6.559	0.467
DBTD6	4.797	2.666	3.732	1.066	−3.731	6.534	0.469

[a]Units are in eV.

electrons. These characteristics, which are closely connected to the energies of HOMO and LUMO, are used to define the electron-accepting capacity of the molecule under investigation. The compounds with higher values of these parameters are considered kinetically more stable and less reactive.[53,54] The chemical (μ) and hardness (η) factors have a direct impact on the energy gap. The negative results of μ demonstrate that the species under investigation are stable enough. In the field of experimental study, particularly in the biological activity of chemicals, these encouraging results may be crucial.[55,56] According to Table 2, the reference chemical outperforms all of the derivatives in terms of electron affinity, electronegativity, and electrophilicity. The donor moiety effectively transfers the electronic charge density to the acceptor since **DBTR** has the maximum IP value (5.937 eV) among all of the described compounds, whereas **DBTD1−DBTD6** have the lowest IP values. The descending order of IP of all of the examined species is **DBTR** > **DBTD1** > **DBTD2** > **DBTD3** > **DBTD4** > **DBTD5** > **DBTD6**. Furthermore, the abovementioned electronegativity values are found to be higher as compared to the electron affinity values. The global hardness values of the derivatives are obtained at a higher level (1.535−1.066 eV) than global softness (0.325−0.469 eV). Interestingly, the highest value of softness is illustrated by **DBTD6** (0.469 eV), and it is considered to be more polarizable than the other chromophores. Thus, all of the evidence designates that **DBTD6** would depict substantial NLO properties.

Natural Bonding Orbital (NBO). NBO analysis is one of the most precise methods for determining electronic charge transfer from the valence band to the conduction band as well as bond interaction and hyperconjugation interaction.[57,58] To study charge transmission in **DBTR** and **DBTD1−DBTD6**, NBO analysis is performed. The π-spacer is employed to transfer charge from a fully occupied donor to an acceptor. By using the second-order perturbation approach, the delocalization of electrons is determined; however, for every donor (i) to acceptor (j) transition, the stabilization energy $E^{(2)}$ is accomplished by delocalization $i \rightarrow j$ and is calculated by using eq 8.

$$E^{(2)} = \Delta E_{ij} = q_i \frac{(F_{i,j})^2}{(E_j - E_i)} \tag{8}$$

Equation 8 describes q_i as the donor occupancy, $F(i, j)$ represents the off-diagonal NBO Fock matrix elements, and E_j and E_i denote the diagonal elements.[59] The higher the stabilization energy, the greater the interaction between donor and acceptor species.[60,61] The results of NBOs for **DBTR** and **DBTD1−DBTD6** are shown in Tables S23−S29.

Overlapping of orbitals results in various hyperconjugative interactions such as $\sigma \rightarrow \sigma^*$, $\pi \rightarrow \pi^*$, LP $\rightarrow \pi^*$, and LP $\rightarrow \sigma^*$ (Tables S23−S29). The most obvious transitions are from $\pi \rightarrow \pi^*$ and the less significant are LP $\rightarrow \pi^*$ and LP $\rightarrow \sigma^*$ and the least dominant are $\sigma \rightarrow \sigma^*$. It is vindicated that the topmost values of $\pi \rightarrow \pi^*$ transition of the **DBTDR**, **DBTD1**, and **DBTD2** occur at 24.62, 40.33, and 28.63 kcal mol^{-1} for π(C38−C40) $\rightarrow$ π^*(C44−C45), π(C1−C2) $\rightarrow$ π^*(C3−C4), and π(C5−C6) $\rightarrow$ π^*(C3−C4), respectively. The bottommost values of stabilization energies are detected as 0.67, 0.77, and 0.52 kcal mol^{-1} for reference (**DBTDR**) and computed compounds (**DBTD1** and **DBTD2**) for π(C49−O63) $\rightarrow$ π^*(C49−O63), π(C80−C82) $\rightarrow$ π^*(C76−C78), and π(C5−C6) $\rightarrow$ π^*(C5−C6), respectively.

The highest values of stabilization energies for $\sigma \rightarrow \sigma^*$ occur as 10.8, 273.77, and 10.86 kcal mol^{-1} of σ(C44−H46) $\rightarrow$ σ^*(C45−S47), σ(C1−C2) $\rightarrow$ σ^*(C1−C6), and σ(N97−C102) $\rightarrow$ σ^*(C98−H99) for **DBTR**, **DBTD1**, and **DBTD2**, respectively, and the lowest values of the same kind of transition occur as 0.5, 0.7, and 0.51 kcal mol^{-1} of σ(C44−H46) $\rightarrow$ σ^*(C45−C48), σ(C90−H93) $\rightarrow$ σ^*(C82−N85), and σ(N97−C102) $\rightarrow$ σ^*(C98−H99), respectively. Furthermore, the highest values of LP $\rightarrow \pi^*$ are calculated as 49.37, 0.69, and 77.15 kcal mol^{-1} of LP(N51) $\rightarrow$ π^*(C54−S65), LP(S30) $\rightarrow$ π^*(C28−C29), and LP(N40) $\rightarrow$ π^*(C41−S43), and the highest values for LP $\rightarrow \sigma^*$ transition observed as 25.87, 0.7, and 30.86 kcal mol^{-1} of LP(O63) $\rightarrow$ σ^*(C49−N51), LP(S30) $\rightarrow$ σ^*(C28−C29), and LP(O42) $\rightarrow$ σ^*(C39−N40) for the reference and designed compounds (**DBTD1** and **DBTD2**), respectively.

In the computed compounds **DBTD3**, **DBTD4**, **DBTD5**, and **DBTD6**, the topmost values of stabilization energies of $\pi \rightarrow \pi^*$ interaction occur as 29.19, 29.26, 326.86, and 323.24 kcal mol^{-1} of π(C5−C6) $\rightarrow$ π^*(C3−C4), π(C5−C6) $\rightarrow$ π^*(C3−C4), π(C125−C126) $\rightarrow$ π^*(C128−C132), and π(C137−C138) $\rightarrow$ π^*(C140−C144). Moreover, the bottommost values of the same transition are observed as 0.5, 0.51, 0.55, and 0.51 kcal mol^{-1} of π(C3−C4) $\rightarrow$ π^*(C3−C4), π(C3−C4) $\rightarrow$ π^*(C3−C4), π(C135−C137) $\rightarrow$ π^*(C135−C137), and π(C3−C4) $\rightarrow$ π^*(C3−C4), respectively. Many other kinds of electronic transitions are defined in the supplementary data (Tables S23−S29).

For the least significant $\sigma \rightarrow \sigma^*$ transition, the highest values of stabilization energies for **DBTD3−DBTD6** are 10.88, 10.91, 8.32, and 10.89 kcal mol^{-1} for σ(C35−H37) $\rightarrow$ σ^*(C36−S38), σ(C35−H37) $\rightarrow$ σ^*(C36−S38), σ(C35−H37) $\rightarrow$ σ^*(S30−C33), and σ(C35−H37) $\rightarrow$ σ^*(C36−S38), whereas the lowest values of the same kind of transition are detected as 0.51, 0.5, 0.51, and 0.52 kcal mol^{-1} of σ(N121−C122) $\rightarrow$ σ^*(C126−H127), σ(C19−C24) $\rightarrow$ σ^*(C24−H26), σ(C113−C114) $\rightarrow$ σ^*(C108−N113), and σ(C77−C79) $\rightarrow$ σ^*(C72−N75), accordingly.

https://doi.org/10.1021/acsomega.3c01472
ACS Omega 2023, 8, 22673−22683

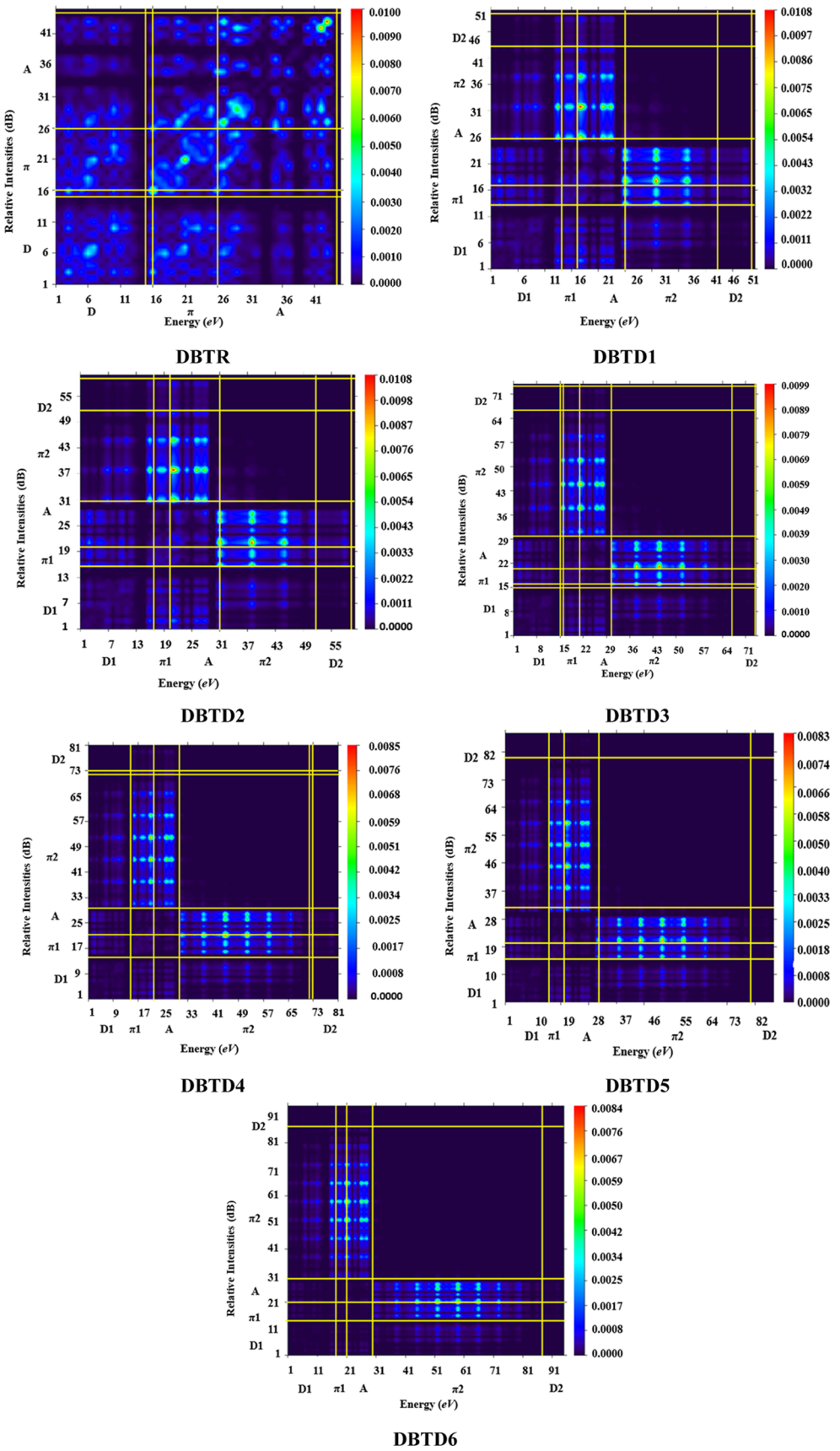

Figure 4. TDM heat maps of **DBTR** and **DBTD1**−**DBTD6**.

The maximum values of slightly significant transition LP → π^* occur as 77.17, 77.16, 77.22, and 77.23 kcal mol^{-1} of LP(N40) → π^*(C41−S43), LP(N40) → π^*(C41−S43), LP(N40) → π^*(C41−S43), and LP(N40) → π^*(C41−S43)

https://doi.org/10.1021/acsomega.3c01472
ACS Omega 2023, 8, 22673−22683

for **DBTD3−DBTD6**, accordingly (Tables S23−S29). For LP → σ^* transition, the observed values of energies are 30.88, 30.85, 30.86, and 30.86 kcal mol^{-1} of LP(O42) → σ^*(C39−N40), LP(O42) → σ^*(C39−N40), LP(O42) → σ^*(C39−N40), and LP(O42) → σ^*(C39−N40) for **DBTD3−DBTD6**, correspondingly. NBO investigation predicts that strong charge transfer and hyperconjugation perform a significant role in stabilizing the designed chromophores in addition to enhancing NLO efficiency.

Natural Population Analysis (NPA) and Molecular Electrostatic Potential (MEP). Mulliken charges are essential in the quantum chemical simulation of the entitled chromophores. The chemical reactivity, dipole moment, and electromagnetic spectra are directly linked to the atomic charges of compounds as mentioned in the literature.[62] For a better understanding of chemical systems, it is essential to understand the atomic charge distribution over the whole chromophore. Moreover, MEP analysis also investigates the charge sites within the compound. The different colors on the MEP surface represent different electrostatic potential values; for example, the red color in the MEP map represents a negative charge area, whereas the green and blue colors represent a positive charge area. The escalating trend of potential is red < orange < yellow < green < blue. The electrophile mostly attacks on the maximum negative area, whereas the nucleophilic attack most likely occurs on the positive region. MEP epitomizes the complete electronic and nuclear charge dissemination of a molecule and is very helpful to analyze the reactive nature of the molecule. The Mulliken charge distribution of **DBTR** and **DBTD1−DBTD6** is displayed in Figure S2. The Mulliken population analysis depicts the imbalanced distribution of atomic charges over the whole molecule because of sulfur and nitrogen atoms. The unequal distribution of charges also has a significant influence on intermolecular and intramolecular interactions. Furthermore, it is also observed that the positive charges are distributed above the hydrogen atoms and negative charges are primarily located on the carbon atoms in all of the examined molecules. Consequently, sulfur atoms have a positive charge, whereas nitrogen atoms have a negative charge. The MEP analysis of **DBTR** and **DBTD1−DBTD6** is accomplished to elucidate the chemical reactivity of compounds (Figure S5). We noticed that the enormous negative potential is dispersed on the nitrogen, sulfur, and oxygen atoms in all of the moieties. The comprehensive delocalization of electrons over the structure is verified by the predominance of green color on the compounds. The nucleophilic and electrophilic positions deliver evidence about the zone from where the molecule has inter or intramolecular interactions. Hence, it is shown that the molecules have a higher shift in charge density, signifying that these designed moieties are more appropriate for promising charge transformation reactions.

Transition Density Matrix (TDM). TDM analysis is considered an excellent tool for the measurement and transmission of electronic density in the excited state. In any molecular system, the TDM analysis presents 3-D heat maps that illustrate the scattering of charge carriers and permit one to detect their coherence as well as delocalization.[63] TDM heat maps for absorption and emission from S_0 to S_1 state of entitled compounds (**DBTR−DBTD6**) are evaluated in the vacuum and shown in Figure 4. It helps to study the donor−acceptor interaction in the excited state and localization of electron holes. The hydrogen atoms are excluded during computation because of their extremely small contribution to transition. The reference molecule is split into three parts, i.e., A, π-spacer, and D, while the derivatives are divided into five fragments, i.e., A_1, π_1, D_1, π_2, and D_2, to draw the TDM graphs. The π-linker serves as a path for charge transfer by providing interactions between donor and acceptor assemblies. The TDM pictographs illustrate that in all of the entitled molecules, there is a good diagonal transference of charge coherence from the donor to the acceptor via π-spacer.

Binding Energy (E_b). Binding energy (E_b) is the most accurate way to check out the optoelectronic features and exciton dissociation potential. It is the difference between the E_{HOMO}/E_{LUMO} band gap (E_{L-H}) and the minimum energy that is needed for the first excitation (E_{opt}).[64] The E_b of examined molecules is computed by utilizing eq 9.

$$E_b = E_{L-H} - E_{opt} \quad (9)$$

In the above equation, E_b represents the binding energy, E_{L-H} is the energy difference, and E_{opt} describes the energy required for the first excitation, while the electron and hole pair is generated. Theoretically calculated binding energies of **DBTR** and **DBTD1−DBTD6** are shown in Table 3.

Table 3. Calculated E_{L-H}, First Singlet Excitation Energy (E_{opt}), and Binding Energy (E_b)[a]

compounds	E_{L-H}	E_{opt}	E_b
DBTR	3.070	2.436	0.634
DBTD1	2.497	2.175	0.322
DBTD2	2.359	2.097	0.262
DBTD3	2.222	2.010	0.212
DBTD4	2.196	2.014	0.182
DBTD5	2.138	1.966	0.172
DBTD6	2.131	1.980	0.151

[a]Units in eV.

The binding energy of **DBTR** is 0.634 eV, whereas the E_b values of designed compounds (**DBTD1−DBTD6**) are 0.322, 0.262, 0.212, 0.182, 0.172, and 0.151 eV, respectively, which are lower than the reference molecule. A gradual decrease in binding energy values is observed among all of the investigated molecules. The reducing order of E_b of the studied compounds is **DBTR > DBTD1 > DBTD2 > DBTD3 > DBTD4 > DBTD5 > DBTD6**. It has been discovered that compounds with an E_b value of 1.9 eV are the best candidates for optical activity. Amusingly, all of the designed derivatives have a lower value of E_b than 1.9 eV and were found to be suitable for the optical activity and various other NLO applications.

Nonlinear Optics (NLO). Significant research is being carried out in nonlinear optics due to its broad range of applications in optoelectronics and telecommunications.[65−67] Owing to their synthetic flexibility and large hyperpolarizability, organic molecules comprising donor and acceptor moieties with a π-conjugative system are widely investigated in comparison to inorganic materials.[68] The computational and experimental fields are granting multidisciplinary activities for the development of NLO active species owing to their optoelectronic modulation, optical signal processing, and superior data rates.[69] Optical analyses such as linear polarizability (α) and nonlinear response (second- and third-order polarizability (β and γ)) of the designed chromophores are determined through electronic characteristics to assess the impact of different π-linkers. The outcomes of μ, $\langle\alpha\rangle$, β_{tot}, and γ_{tot} were computed at the aforesaid basis set and level of DFT, and the main results are shown in

https://doi.org/10.1021/acsomega.3c01472
ACS Omega 2023, 8, 22673−22683

Table 4, while their contributing tensors are tabulated in Tables S30−S33.

Table 4. Average Polarizability $\langle\alpha\rangle$, Dipole Moment (μ), First Hyperpolarizability (β_{tot}), Second-Order Hyperpolarizability (γ_{tot}), and Major Donating Tensors (esu) for (DBTR and DBTD1−DBTD6) Molecules in esu

compounds	μ_{tot}	$\langle\alpha\rangle \times 10^{-22}$	$\beta_{tot} \times 10^{-29}$	$\gamma_{tot} \times 10^{-32}$
DBTR	7.5202	1.446	0.072	0.734
DBTD1	11.130	1.502	0.903	0.896
DBTD2	9.630	1.678	0.936	1.037
DBTD3	11.350	2.019	1.019	1.116
DBTD4	11.401	2.194	1.008	1.122
DBTD5	12.597	2.378	1.140	1.331
DBTD6	12.855	2.533	0.997	1.121

The dipole moment is observed due to the electronegativity (E.N) difference and is directly associated with it, i.e., the larger the E.N difference, the greater would be the dipole moment.[70] Moreover, the polarity of the molecule also influences dipole moment by escalating their nonlinear values.[71] The data shown in Table S32 reveals that the dipole moment is more dominant along the x-axis in all of the computed molecules. The magnitude of μ_{xx} tensor is found to be the highest in **DBTD6**, which is 11.888 D (Table S32). The decreasing order of μ_{tot} for the studied molecules is **DBTD6** > **DBTD5** > **DBTD4** > **DBTD3** > **DBTD1** > **DBTD2** > **DBTR**. The values of $\langle\alpha\rangle$ are used to describe the linear response. The observed $\langle\alpha\rangle$ values of **DBTR** and **DBTD1−DBTD6** are 1.446×10^{-22}, 1.502×10^{-22}, 1.678×10^{-22}, 2.019×10^{-22}, 2.194×10^{-22}, 2.378×10^{-22}, and 2.533×10^{-22} esu, respectively (Tables S31 and 4). The declining order of $\langle\alpha\rangle$ of all of the computed species is observed as **DBTD6** > **DBTD5** > **DBTD4** > **DBTD3** > **DBTD2** > **DBTD1** > **DBTR**. Like μ_{tot}, the highest value of α_{tot} is noticed in **DBTD6**, which is due to the increase in conjugation.

For second hyperpolarizability, the main contribution to β_{tot} is due to β_{xxx} tensor with a magnitude of 9.658×10^{-28} esu in **DBTD5**, which indicates that a significant amount of charge transfer is observed from donor to acceptor via π-bridge along the x-axis (Table S30). The highest computed value of β_{tot} is noted in **DBTD5**, which is 1.140×10^{-27} esu and is much greater than the urea molecule (β for urea is 0.3728×10^{-30} esu). The remarkably higher value of β_{tot} of **DBTD5** might be due to the good donor moiety, which enhances the push−pull mechanism and the seven aniline π-linkers, which have an eminent effect on conjugation. γ_{tot} is one of the main factors used to estimate the NLO response. Among all of the computed molecules, the largest value of γ_{tot} is noted in **DBTD5**, which is 1.331×10^{-32} esu. γ_x tensor is prominent and depicts a larger value than all of the other tensor components (Table S33). From the above discussion, it can be summarized that the x-axis mainly contributes to intramolecular charge transfer more than other axes, and all of the investigated compounds exhibit greater potential for NLO applications with higher hyperpolarizability values.

CONCLUSIONS

In this study, we explored NLO characteristics of hypothetically designed compounds (**DBTD1−DBTD6**) from **DBTR** to discover highly competent NLO material. The effect of changing the π-linker and donor was noticed for NLO response, and the outcomes illustrated that it has a significant influence over A−π_1−D_1−π_2−D_2 architecture. Interestingly, a reduced energy difference was noticed in the range of 3.070−2.131 eV (**DBTD1−DBTD6**) with a wider absorption spectrum than the reference. The lowest value of the band gap was noted in **DBTD6**, which is 2.131 eV. The GRP data disclosed that increased conjugation in chromophores gives extraordinary stability to all of the studied compounds, whereas the highest softness value was seen in **DBTD6**. Furthermore, **DBTD5** exhibits a bathochromic shift with the highest λ_{max} values of 593.425 and 630.578 nm along with 2.089 and 1.966 eV transition energy values in both gaseous and solvent phases, respectively. The lowest binding energy value of 0.151 eV in **DBTD6** reveals that the molecule has the highest power conversion efficiency (PCE). Moreover, the NBO study exposes that the most prominent transition along with the largest value of stabilization energy (326.86 kcal mol^{-1}) was observed in **DBTD5**. All of the titled derivatives exhibit a greater dipole moment (μ = 11.130−12.855 D) than the reference compound, which shows their better polarizability and resulted in a fascinating NLO response. A remarkable β_{tot} and $\langle\gamma\rangle$ values of 1.140×10^{-27} and 1.331×10^{-32} esu, correspondingly, were noted in **DBTD5**, which demonstrated that it exhibits auspicious second- and third-order NLO properties. Thus, it can be summarized that our work would give valuable insight for experimentalists to discover these alluring NLO materials.

COMPUTATIONAL PROCEDURES

Density functional theory (DFT) and time-dependent density functional theory (TD-DFT) analyses were accomplished to acquire the absorption spectrum, electronic, and NLO characteristics of **DBTR** and **DBTD1−DBTD6**. Gaussian 09 program[72] was utilized to perform the quantum chemical calculations at the M06/6-311G(d,p) level of theory,[73,74] and the results were visualized by utilizing the GaussView 6.0 program.[75] For UV−visible and FMO analyses, the TD-DFT approach was employed to evaluate the electronic transitions and compute the energy gap between HOMO and LUMO. The NBO, FMO, GRP, MEP, NPA, NLO, and TDM analyses were conducted at the aforementioned level of theory in solvent (chloroform) media. Moreover, for the elucidation of output results, ChemCraft,[76] Origin 8.0,[77] Avogadro,[78] and Multiwfn 3.7 program[79] packages were employed. The dipole moment was calculated from eq 10.[80]

$$\mu = (\mu_x^2 + \mu_y^2 + \mu_z^2)^{1/2} \tag{10}$$

Average linear polarizability $\langle a\rangle$ was evaluated using eq 11.[81]

$$\langle a\rangle = 1/3(a_{xx} + a_{yy} + a_{zz}) \tag{11}$$

The magnitude of the first hyperpolarizability was measured by utilizing eq 12.[82]

$$\beta_{tot} = [(\beta_{xxx} + \beta_{xyy} + \beta_{xzz})^2 + (\beta_{yyy} + \beta_{yzz} + \beta_{yxx})^2 + (\beta_{zzz} + \beta_{zxx} + \beta_{xyz})^2]^{1/2} \tag{12}$$

Moreover, the values of second hyperpolarizability $\langle\gamma\rangle$ were estimated by using eq 13.[83]

$$\gamma_{tot} = \sqrt{\gamma_x^2 + \gamma_y^2 + \gamma_z^2} \tag{13}$$

https://doi.org/10.1021/acsomega.3c01472
ACS Omega 2023, 8, 22673−22683

■ ASSOCIATED CONTENT

Supporting Information

The Supporting Information is available free of charge at https://pubs.acs.org/doi/10.1021/acsomega.3c01472.

Cartesian coordinates of DBTR and **DBTD1−DBTD6**; calculated energy (E) and energy gap (ΔE) of entitled compounds; NBO and UV−vis data (wavelength, excitation energies, and oscillator strengths) of investigated compounds; FMOs of **DBTR** and **DBTD1−DBTD6**; dipole moment, dipole polarizability, and IUPAC names of the studied compounds; and NLO of reported chromophores was calculated using the M06/6-31G (d,p) method. (PDF)

■ AUTHOR INFORMATION

Corresponding Author

Faiz Rasool − *Institute of Chemical Sciences, Bahauddin Zakariya University, Multan 60800, Pakistan;* orcid.org/0000-0002-7825-9667; Email: faizrasoolbzu@gmail.com

Authors

Ghulam Mustafa − *Institute of Chemical Sciences, Bahauddin Zakariya University, Multan 60800, Pakistan*

Iqra Shafiq − *Institute of Chemistry, Khwaja Fareed University of Engineering & Information Technology, Rahim Yar Khan 64200, Pakistan; Centre for Theoretical and Computational Research, Khwaja Fareed University of Engineering & Information Technology, Rahim Yar Khan 64200, Pakistan*

Qurat-ul-ain Shaikh − *Institute of Chemistry, Shah Abdul Latif University Khairpur, Khairpur 66111, Pakistan*

Ayesha Mustafa − *Institute of Chemistry, Khwaja Fareed University of Engineering & Information Technology, Rahim Yar Khan 64200, Pakistan; Centre for Theoretical and Computational Research, Khwaja Fareed University of Engineering & Information Technology, Rahim Yar Khan 64200, Pakistan*

Romaisa Zahid − *Institute of Chemistry, Khwaja Fareed University of Engineering & Information Technology, Rahim Yar Khan 64200, Pakistan; Centre for Theoretical and Computational Research, Khwaja Fareed University of Engineering & Information Technology, Rahim Yar Khan 64200, Pakistan*

Muhammad Adnan Asghar − *Department of Chemistry, Division of Science and Technology, University of Education Lahore, Lahore 54770, Pakistan*

Rabia Baby − *Department of education, Sukkur IBA University, Sukkur 65200 Sindh, Pakistan*

Saad M. Alshehri − *Department of Chemistry, College of Science, King Saud University, Riyadh 11451, Saudi Arabia*

Muhammad Haroon − *Department of Chemistry and Biochemistry, Miami University, Oxford, Ohio 45056, United States*

Complete contact information is available at: https://pubs.acs.org/10.1021/acsomega.3c01472

Notes

The authors declare no competing financial interest.

■ ACKNOWLEDGMENTS

The authors thank the Researchers Supporting Project number (RSP2023R29), King Saud University, Riyadh, Saudi Arabia.

■ REFERENCES

(1) Boyd, R. W. *Nonlinear Optics*; Academic Press: San Diego, 1992; Vol. *155*.

(2) Zafar, F.; Mehboob, M. Y.; Hussain, R.; Khan, M. a. U.; Hussain, A.; Hassan, T.; Rashid, M.; Shahi, M. N. End-Capped Engineering of Truxene Core Based Acceptor Materials for High Performance Organic Solar Cells: Theoretical Understanding and Prediction. *Opt. Quantum Electron.* **2021**, *53*, 1−24.

(3) Shi, Y.; Zhang, C.; Zhang, H.; Bechtel, J. H.; Dalton, L. R.; Robinson, B. H.; Steier, W. H. Low (Sub-1-Volt) Halfwave Voltage Polymeric Electro-Optic Modulators Achieved by Controlling Chromophore Shape. *Science* **2000**, *288*, 119−122.

(4) Muhammad, S.; Kumar, S.; Koh, J.; Saravanabhavan, M.; Ayub, K.; Chaudhary, M. Synthesis, Characterisation, Optical and Nonlinear Optical Properties of Thiazole and Benzothiazole Derivatives: A Dual Approach. *Mol. Simul.* **2018**, *44*, 1191−1199.

(5) Halasyamani, P. S.; Zhang, W. Inorganic Materials for UV and Deep-UV Nonlinear-Optical Applications. In *Inorganic Chemistry*; ACS Publications, 2017; pp 12077−12085.

(6) Yamashita, S. A Tutorial on Nonlinear Photonic Applications of Carbon Nanotube and Graphene. *J. Lightwave Technol.* **2012**, *30*, 427−447.

(7) Guo, L.; Guo, Z.; Li, X. Design and Preparation of Side Chain Electro-Optic Polymeric Materials Based on Novel Organic Second Order Nonlinear Optical Chromophores with Double Carboxyl Groups. *J. Mater. Sci.: Mater. Electron.* **2018**, *29*, 2577−2584.

(8) Chen, W.; Tian, K.; Song, X.; Zhang, Z.; Ye, K.; Yu, G.; Wang, Y. Large π-Conjugated Quinacridone Derivatives: Syntheses, Characterizations, Emission, and Charge Transport Properties. *Org. Lett.* **2015**, *17*, 6146−6149.

(9) Wang, C.; Zhang, Z.; Wang, Y. Quinacridone-Based π-Conjugated Electronic Materials. *J. Mater. Chem. C* **2016**, *4*, 9918−9936.

(10) Fu, G.; Yoda, T.; Kasatani, K.; Okamoto, H.; Takenaka, S. Third-Order Optical Nonlinearities of Naphthalocyanine Derivatives Measured by Resonant Femtosecond Degenerate Four-Wave Mixing Technique. *Synth. Met.* **2005**, *155*, 68−72.

(11) Mahmood, A.; Khan, S. U.-D.; Rana, U. A.; Tahir, M. H. Red Shifting of Absorption Maxima of Phenothiazine Based Dyes by Incorporating Electron-Deficient Thiadiazole Derivatives as π-Spacer. *Arabian J. Chem.* **2019**, *12*, 1447−1453.

(12) Zhu, G.; Luo, W.; Wang, L.; Jiang, W.; Yang, J. Silicon: Toward Eco-Friendly Reduction Techniques for Lithium-Ion Battery Applications. *J. Mater. Chem. A* **2019**, *7*, 24715−24737.

(13) Wild, S.; Tice, N. DFT Study of Structural and Electronic Properties of 1, 4-Diarylcyclopenta [d] Pyridazines and Oxazines for Non-Linear Optical Applications. *J. Mol. Model.* **2021**, *27*, No. 60.

(14) Hutton, J.; Jones, A. D.; Lee, S. A.; Martin, D. M.; Meyrick, B. R.; Patel, I.; Peardon, R. F.; Powell, L. Use of a Titanium Thienyl Anion and a Simple Procedure for Introducing a Thiol Group into Thiophene in the Development of a Manufacturing Route to the 5-Lipoxygenase Inhibitor ZD4407. *Org. Process Res. Dev.* **1997**, *1*, 61−67.

(15) Ong, B. S.; Wu, Y.; Li, Y.; Liu, P.; Pan, H. Thiophene Polymer Semiconductors for Organic Thin-Film Transistors. *Chem. - Eur. J.* **2008**, *14*, 4766−4778.

(16) Fujinami, Y.; Kuwabara, J.; Lu, W.; Hayashi, H.; Kanbara, T. Synthesis of Thiophene-and Bithiophene-Based Alternating Copolymers via Pd-Catalyzed Direct C−H Arylation. *ACS Macro Lett.* **2012**, *1*, 67−70.

(17) Alharthy, R. D.; Ahmed, N.; Mubarak, S.; Yaqub, M.; Khalid, M.; Shafiq, I.; Asghar, M. A.; Braga, A. A. C.; Shafiq, Z. Design, Synthesis, and Density Functional Theory Studies of Indole Hydrazones as Colorimetric "Naked Eye" Sensors for F Ions. *ACS Omega* **2023**, *8*, 14131−14143.

(18) Bratcher, M. S.; DeClue, M. S.; Grunnet-Jepsen, A.; Wright, D.; Smith, B. R.; Moerner, W. E.; Siegel, J. S. Synthesis of Bifunctional Photorefractive Polymers with Net Gain: Design Strategy Amenable to Combinatorial Optimization. *J. Am. Chem. Soc.* **1998**, *120*, 9680−9681.

(19) Abeyasinghe, N.; de Silva, R. M.; de Silva, K. N. Non-Linear Optical (NLO) Properties of Conjugated Thiophene and Ethylene

Dioxy Thiophene (EDOT) Oligomers: A Density Functional Theory (DFT) Study. *Int. Res. J. Pure Appl. Chem.* **2016**, *13*, 1−11.
(20) Hagen, R.; Bieringer, T. Photoaddressable Polymers for Optical Data Storage. *Adv. Mater.* **2001**, *13*, 1805−1810.
(21) Kanis, D. R.; Ratner, M. A.; Marks, T. J. Design and Construction of Molecular Assemblies with Large Second-Order Optical Nonlinearities. Quantum Chemical Aspects. *Chem. Rev.* **1994**, *94*, 195−242.
(22) AlFaify, S.; Shkir, M.; Arora, M.; Irfan, A.; Algarni, H.; Abbas, H.; Al-Sehemi, A. G. Quantum Chemical Investigation on Molecular Structure, Vibrational, Photophysical and Nonlinear Optical Properties of l-Threoninium Picrate: An Admirable Contender for Nonlinear Applications. *J. Comput. Electron.* **2018**, *17*, 1421−1433.
(23) Williams, D. J. Non-Linear Optical Properties of Organic Materials. *Thin Solid Films* **1992**, *216*, 117−122.
(24) Prasad, P. N.; Williams, D. J. *Introduction to Nonlinear Optical Effects in Molecules and Polymers*; Wiley: New York, 1991; Vol. *1*.
(25) Khalid, M.; Ali, A.; Jawaria, R.; Asghar, M. A.; Asim, S.; Khan, M. U.; Hussain, R.; ur Rehman, M. F.; Ennis, C. J.; Akram, M. S. First Principles Study of Electronic and Nonlinear Optical Properties of A−D−π−A and D−A−D−π−A Configured Compounds Containing Novel Quinoline−Carbazole Derivatives. *RSC Adv.* **2020**, *10*, 22273−22283.
(26) Zhang, Y.; Wang, H.; Ye, J.; Qiu, Y. Redox-Triggered Switch Based on Platinum (Ii) Acetylacetonate Complexes Bearing an Isomeric Donor−Acceptor Conjugation Ligand Shows a High Second-Order Nonlinear Optical Response. *New J. Chem.* **2019**, *43*, 11263−11274.
(27) Coe, B. J.; Harris, J. A.; Brunschwig, B. S.; Asselberghs, I.; Clays, K.; Garín, J.; Orduna, J. Three-Dimensional Nonlinear Optical Chromophores Based on Metal-to-Ligand Charge-Transfer from Ruthenium (II) or Iron (II) Centers. *J. Am. Chem. Soc.* **2005**, *127*, 13399−13410.
(28) Castet, F.; Rodriguez, V.; Pozzo, J.-L.; Ducasse, L.; Plaquet, A.; Champagne, B. Design and Characterization of Molecular Nonlinear Optical Switches. *Acc. Chem. Res.* **2013**, *46*, 2656−2665.
(29) Shehzadi, K.; Ayub, K.; Mahmood, T. Theoretical Study on Design of Novel Superalkalis Doped Graphdiyne: A New Donor−Acceptor (D-π-A) Strategy for Enhancing NLO Response. *Appl. Surf. Sci.* **2019**, *492*, 255−263.
(30) Kohlman, R. S.; Epstein, A. J.Insulator-Metal Transition and Inhomogeneous Metallic State in Conducting Polymers. In *Handbook of Conducting Polymers*; Marcel Dekker Inc., 1998; Vol. *2*, pp 85−122.
(31) Kaneto, K.; Yoshino, K.; Inuishi, Y. Electrical and Optical Properties of Polythiophene Prepared by Electrochemical Polymerization. *Solid State Commun.* **1983**, *46*, 389−391.
(32) Sone, T.; Sato, K.; Ohba, Y. Synthesis and Reductive Desulfurization of Crown Ethers Containing Thiophene Subunit. *Bull. Chem. Soc. Jpn.* **1989**, *62*, 838−844.
(33) Kim, Y.; Song, C. E.; Moon, S.-J.; Lim, E. Rhodanine Dye-Based Small Molecule Acceptors for Organic Photovoltaic Cells. *Chem. Commun.* **2014**, *50*, 8235−8238.
(34) Uzun, S.; Esen, Z.; Koç, E.; Usta, N. C.; Ceylan, M. Experimental and Density Functional Theory (MEP, FMO, NLO, Fukui Functions) and Antibacterial Activity Studies on 2-Amino-4-(4-Nitrophenyl)-5, 6-Dihydrobenzo [h] Quinoline-3-Carbonitrile. *J. Mol. Struct.* **2019**, *1178*, 450−457.
(35) Khalid, M.; Hussain, R.; Hussain, A.; Ali, B.; Jaleel, F.; Imran, M.; Assiri, M. A.; Usman Khan, M.; Ahmed, S.; Abid, S.; et al. Electron Donor and Acceptor Influence on the Nonlinear Optical Response of Diacetylene-Functionalized Organic Materials (DFOMs): Density Functional Theory Calculations. *Molecules* **2019**, *24*, 2096.
(36) Khalid, M.; Ali, A.; Abid, S.; Tahir, M. N.; Khan, M. U.; Ashfaq, M.; Imran, M.; Ahmad, A. Facile Ultrasound-Based Synthesis, SC-XRD, DFT Exploration of the Substituted Acyl-Hydrazones: An Experimental and Theoretical Slant towards Supramolecular Chemistry. *ChemistrySelect* **2020**, *5*, 14844−14856.
(37) Khalid, M.; Ali, A.; Adeel, M.; Din, Z. U.; Tahir, M. N.; Rodrigues-Filho, E.; Iqbal, J.; Khan, M. U. Facile Preparation, Characterization, SC-XRD and DFT/DTDFT Study of Diversely Functionalized Unsymmetrical Bis-Aryl-α, β-Unsaturated Ketone Derivatives. *J. Mol. Struct.* **2020**, *1206*, No. 127755.
(38) Sarwar, S.; Yaqoob, J.; Khan, M. U.; Hussain, R.; Zulfiqar, S.; Anwar, A.; Assiri, M. A.; Imran, M.; Ibrahim, M. M.; Mersal, G. A.; Elnaggar, A. Y. Deciphering the Role of Alkali Metals (Li, Na, K) Doping for Triggering Nonlinear Optical (NLO) Properties of T-Graphene Quantum Dots: Toward the Development of Giant NLO Response Materials. *ACS Omega* **2022**, *7*, 24396−24414.
(39) Arif, N.; Shafiq, Z.; Noureen, S.; Khalid, M.; Ashraf, A.; Yaqub, M.; Irshad, S.; Khan, M. U.; Arshad, M. N.; Braga, A. A. C.; et al. Synthesis, Spectroscopic, SC-XRD/DFT and Non-Linear Optical (NLO) Properties of Chromene Derivatives. *RSC Adv.* **2022**, *13*, 464−477.
(40) Khalid, M.; Imran, M.; Braga, A. A. C.; Akram, M. S.; et al. Molecular Engineering of Indenoindene-3-Ethylrodanine Acceptors with A2-A1-D-A1-A2 Architecture for Promising Fullerene-Free Organic Solar Cells. *Sci. Rep.* **2021**, *11*, No. 20320.
(41) Khalid, M.; Ali, M.; Aslam, M.; Sumrra, S. H.; Khan, M. U.; Raza, N.; Kumar, N.; Imran, M. Frontier Molecular, Natural Bond Orbital, UV-Vis Spectral Stduy, Solvent Influence on Geometric Parameters, Vibrational Frequencies and Solvation Energies of 8-Hydroxyquinoline. *Int. J. Pharm. Sci. Res.* **2017**, *8*, 457−469.
(42) Prashanth, J.; Ramesh, G.; Naik, J. L.; Ojha, J. K.; Reddy, B. V. Molecular Geometry, NBO Analysis, Hyperpolarizability and HOMO-LUMO Energies of 2-Azido-1-Phenylethanone Using Quantum Chemical Calculations. *Mater. Today: Proc.* **2016**, *3*, 3761−3769.
(43) Khalid, M.; Khan, M. U.; Shafiq, I.; Hussain, R.; Mahmood, K.; Hussain, A.; Jawaria, R.; Hussain, A.; Imran, M.; Assiri, M. A.; et al. NLO Potential Exploration for D−π−A Heterocyclic Organic Compounds by Incorporation of Various π-Linkers and Acceptor Units. *Arabian J. Chem.* **2021**, *14*, No. 103295.
(44) Khalid, M.; Khan, M.; Mahmood, K.; Arshad, M.; Imran, M.; Braga, A. A. C.; Hussain, R. Theoretical Designing of Non-Fullerene Derived Organic Heterocyclic Compounds with Enhanced Nonlinear Optical Amplitude: A DFT Based Prediction. *Sci. Rep.* **2022**, *12*, No. 20220.
(45) Lee, J.; Lee, S. M.; Chen, S.; Kumari, T.; Kang, S.-H.; Cho, Y.; Yang, C. Organic Photovoltaics with Multiple Donor−Acceptor Pairs. *Adv. Mater.* **2019**, *31*, No. 1804762.
(46) Khan, M. U.; Khalid, M.; Shafiq, I.; Khera, R. A.; Shafiq, Z.; Jawaria, R.; Shafiq, M.; Alam, M. M.; Braga, A. A. C.; Imran, M.; Kanwal, F.; Xu, Z.; Lu, C. Theoretical Investigation of Nonlinear Optical Behavior for Rod and T-Shaped Phenothiazine Based D-π-A Organic Compounds and Their Derivatives. *J. Saudi Chem. Soc.* **2021**, *25*, No. 101339.
(47) Saleem, T.; Khan, S.; Yaqub, M.; Khalid, M.; Islam, M.; ur Rehman, M. Y.; Rashid, M.; Shafiq, I.; Braga, A. A.; Syed, A.; et al. Novel Quinoline-Derived Chemosensors: Synthesis, Anion Recognition, Spectroscopic, and Computational Study. *New J. Chem.* **2022**, *46*, 18233−18243.
(48) Parr, R. G.; Szentpály, Lv.; Liu, S. Electrophilicity Index. *J. Am. Chem. Soc.* **1999**, *121*, 1922−1924.
(49) Parr, R. G.; Donnelly, R. A.; Levy, M.; Palke, W. E. Electronegativity: The Density Functional Viewpoint. *J. Chem. Phys.* **1978**, *68*, 3801−3807.
(50) Chattaraj, P. K.; Roy, D. R. Update 1 of: Electrophilicity Index. *Chem. Rev.* **2007**, *107*, PR46−PR74.
(51) Kovačević, N.; Kokalj, A. Analysis of Molecular Electronic Structure of Imidazole-and Benzimidazole-Based Inhibitors: A Simple Recipe for Qualitative Estimation of Chemical Hardness. *Corros. Sci.* **2011**, *53*, 909−921.
(52) Sheela, N. R.; Muthu, S.; Sampathkrishnan, S. Molecular Orbital Studies (Hardness, Chemical Potential and Electrophilicity), Vibrational Investigation and Theoretical NBO Analysis of 4-4′-(1H-1, 2, 4-Triazol-1-Yl Methylene) Dibenzonitrile Based on Abinitio and DFT Methods. *Spectrochim. Acta, Part A* **2014**, *120*, 237−251.
(53) Ali, A.; Khalid, M.; Marrugo, K. P.; Kamal, G. M.; Saleem, M.; Khan, M. U.; Concepción, O.; Alexander, F. Spectroscopic and DFT/

https://doi.org/10.1021/acsomega.3c01472
ACS Omega 2023, 8, 22673−22683

TDDFT Insights of the Novel Phosphonate Imine Compounds. *J. Mol. Struct.* **2020**, *1207*, No. 127838.
(54) Khalid, M.; Lodhi, H. M.; Khan, M. U.; Imran, M. Structural Parameter-Modulated Nonlinear Optical Amplitude of Acceptor−π−D−π−Donor-Configured Pyrene Derivatives: A DFT Approach. *RSC Adv.* **2021**, *11*, 14237−14250.
(55) Pasha, A. R.; Khalid, M.; Shafiq, Z.; Khan, M. U.; Naseer, M. M.; Tahir, M. N.; Hussain, R.; Braga, A. A. C.; Jawaria, R. A Comprehensive Study of Structural, Non-Covalent Interactions and Electronic Insights into N-Aryl Substituted Thiosemicarbazones via SC-XRD and First-Principles DFT Approach. *J. Mol. Struct.* **2021**, *1230*, No. 129852.
(56) Khalid, M.; Naseer, S.; Tahir, M. S.; Shafiq, I.; Munawar, K. S.; de Alcântara Morais, S. F.; Braga, A. A. A Theoretical Approach towards Designing of Banana Shaped Non-Fullerene Chromophores Using Efficient Acceptors Moieties: Exploration of Their NLO Response Properties. *Opt. Quantum Electron.* **2023**, *55*, No. 258.
(57) Khalid, M.; Khan, M. U.; Shafiq, I.; Hussain, R.; Ali, A.; Imran, M.; Braga, A. A.; Fayyaz ur Rehman, M.; Akram, M. S. Structural Modulation of π-Conjugated Linkers in D−π−A Dyes Based on Triphenylamine Dicyanovinylene Framework to Explore the NLO Properties. *R. Soc. Open Sci.* **2021**, *8*, No. 210570.
(58) Khalid, M.; Khan, M.; Shafiq, I.; Mahmood, K.; Akhtar, M. N.; Iqbal, J.; Assiri, M. A.; Imran, M.; Braga, A. A. C. Role of Donors in Triggering Second Order Non-Linear Optical Properties of Non-Fullerene FCO-2FR1 Based Derivatives: A Theoretical Perspective. *Heliyon* **2023**, *9*, No. e13033.
(59) Reed, A. E.; Curtiss, L. A.; Weinhold, F. Intermolecular Interactions from a Natural Bond Orbital, Donor-Acceptor Viewpoint. *Chem. Rev.* **1988**, *88*, 899−926.
(60) Khalid, M.; Zafar, M.; Hussain, S.; Asghar, M. A.; Khera, R. A.; Imran, M.; Abookleesh, F. L.; Akram, M. Y.; Ullah, A. Influence of End-Capped Modifications in the Nonlinear Optical Amplitude of Nonfullerene-Based Chromophores with a D- π−A Architecture: A DFT/TDDFT Study. *ACS Omega* **2022**, *7*, 23532−23548.
(61) Khalid, M.; Ali, A.; Rehman, M. F. U.; Mustaqeem, M.; Ali, S.; Khan, M. U.; Asim, S.; Ahmad, N.; Saleem, M. Exploration of Noncovalent Interactions, Chemical Reactivity, and Nonlinear Optical Properties of Piperidone Derivatives: A Concise Theoretical Approach. *ACS Omega* **2020**, *5*, 13236−13249.
(62) Khalid, M.; Ali, A.; De la Torre, A. F.; Marrugo, K. P.; Concepcion, O.; Kamal, G. M.; Muhammad, S.; Al-Sehemi, A. G. Facile Synthesis, Spectral (IR, Mass, UV- Vis, NMR), Linear and Nonlinear Investigation of the Novel Phosphonate Compounds: A Combined Experimental and Simulation Study. *ChemistrySelect* **2020**, *5*, 2994−3006.
(63) Li, Y.; Ullrich, C. A. Time-Dependent Transition Density Matrix. *Chem. Phys.* **2011**, *391*, 157−163.
(64) Dkhissi, A. Excitons in Organic Semiconductors. *Synth. Met.* **2011**, *161*, 1441−1443.
(65) Muthu, S.; Maheswari, J. U. Quantum Mechanical Study and Spectroscopic (FT-IR, FT-Raman, 13C, 1H, UV) Study, First Order Hyperpolarizability, NBO Analysis, HOMO and LUMO Analysis of 4-[(4-Aminobenzene) Sulfonyl] Aniline by Ab Initio HF and Density Functional Method. *Spectrochim. Acta, Part A* **2012**, *92*, 154−163.
(66) Govindarasu, K.; Kavitha, E. Vibrational Spectra, Molecular Structure, NBO, UV, NMR, First Order Hyperpolarizability, Analysis of 4-Methoxy-4′-Nitrobiphenyl by Density Functional Theory. *Spectrochim. Acta, Part A* **2014**, *122*, 130−141.
(67) Khalid, M.; Ahmed, R.; Shafiq, I.; Arshad, M.; Asghar, M. A.; Munawar, K. S.; Imran, M.; Braga, A. A. First Theoretical Framework for Highly Efficient Photovoltaic Parameters by Structural Modification with Benzothiophene-Incorporated Acceptors in Dithiophene Based Chromophores. *Sci. Rep.* **2022**, *12*, No. 20148.
(68) Sivaranjani, T.; Xavier, S.; Periandy, S. NMR, FT-IR, FT-Raman, UV Spectroscopic, HOMO−LUMO and NBO Analysis of Cumene by Quantum Computational Methods. *J. Mol. Struct.* **2015**, *1083*, 39−47.
(69) Breitung, E. M.; Shu, C.-F.; McMahon, R. J. Thiazole and Thiophene Analogues of Donor- Acceptor Stilbenes: Molecular Hyperpolarizabilities and Structure- Property Relationships. *J. Am. Chem. Soc.* **2000**, *122*, 1154−1160.
(70) Fukui, K. Role of Frontier Orbitals in Chemical Reactions. *Science* **1982**, *218*, 747−754.
(71) Saeed, A.; Muhammad, S.; Rehman, S.; Bibi, S.; Al-Sehemi, A. G.; Khalid, M. Exploring the Impact of Central Core Modifications among Several Push-Pull Configurations to Enhance Nonlinear Optical Response. *J. Mol. Graphics Modell.* **2020**, *100*, No. 107665.
(72) Frisch, M. J.; Trucks, G. W.; Schlegel, H. B.; Scuseria, G. E.; Robb, M. A.; Cheeseman, J. R.; Scalmani, G.; Barone, V.; Mennucci, B.; Petersson, G. *Gaussian 09*, revision D. 01; Gaussian, Inc.: Wallingford CT. See also: http://www.gaussian.com, 2009.
(73) Andersson, M. P.; Uvdal, P. New Scale Factors for Harmonic Vibrational Frequencies Using the B3LYP Density Functional Method with the Triple-ζ Basis Set 6-311+ G (d, p). *J. Phys. Chem. A* **2005**, *109*, 2937−2941.
(74) Zhao, Y.; Truhlar, D. G. The M06 Suite of Density Functionals for Main Group Thermochemistry, Thermochemical Kinetics, Noncovalent Interactions, Excited States, and Transition Elements: Two New Functionals and Systematic Testing of Four M06-Class Functionals and 12 Other Functionals. *Theor. Chem. Acc.* **2008**, *120*, 215−241.
(75) Dennington, R.; Keith, T. A.; Millam, J. M. *GaussView*; Semichem Inc: Shawnee Mission KS, 2016.
(76) Zhurko, G. A.; Zhurko, D. A. *ChemCraft*, version 1.6. http://www.chemcraftprog.com, 2009.
(77) *OriginPro, V.*; OriginLab Corporation: Northampton, MA, USA, 2016.
(78) Hanwell, M. D.; Curtis, D. E.; Lonie, D. C.; Vandermeersch, T.; Zurek, E.; Hutchison, G. R. Avogadro: An Advanced Semantic Chemical Editor, Visualization, and Analysis Platform. *J. Cheminf.* **2012**, *4*, No. 17.
(79) Lu, T.; Chen, F. Multiwfn: A Multifunctional Wavefunction Analyzer. *J. Comput. Chem.* **2012**, *33*, 580−592.
(80) Hudson, J. J.; Sauer, B. E.; Tarbutt, M. R.; Hinds, E. A. Measurement of the Electron Electric Dipole Moment Using YbF Molecules. *Phys. Rev. Lett.* **2002**, *89*, No. 023003.
(81) Alparone, A. Linear and Nonlinear Optical Properties of Nucleic Acid Bases. *Chem. Phys.* **2013**, *410*, 90−98.
(82) Oudar, J.-L.; Chemla, D. S. Hyperpolarizabilities of the Nitroanilines and Their Relations to the Excited State Dipole Moment. *J. Chem. Phys.* **1977**, *66*, 2664−2668.
(83) Naik, V. S.; Patil, P. S.; Wong, Q. A.; Quah, C. K.; Gummagol, N. B.; Jayanna, H. S. Molecular Structure, Linear Optical, Second and Third-Order Nonlinear Optical Properties of Two Non-Centrosymmetric Thiophene-Chalcone Derivatives. *J. Mol. Struct.* **2020**, *1222*, No. 128901.

https://doi.org/10.1021/acsomega.3c01472
ACS Omega 2023, 8, 22673−22683